**Atmospheric
Chemistry
and Physics
Discussions**

Water content of aged aerosol

G. J. Engelhart[1]**, L. Hildebrandt**[1]**, E. Kostenidou**[2,4]**, N. Mihalopoulos**[3]**,
N. M. Donahue**[1]**, and S. N. Pandis**[1,2,4]

[1]Department of Chemical Engineering, Carnegie Mellon University, Pittsburgh, PA, USA
[2]Department of Chemical Engineering, University of Patras, Patra, Greece
[3]University of Crete, Environmental Chemical Processes Laboratory (ECPL),
Heraklion, Greece
[4]Institute of Chemical Engineering and High Temperature Chemical Processes (ICE-HT),
Foundation of Research and Technology (FORTH), Patra, Greece

Discussion Paper | Discussion Paper | Discussion Paper | Discussion Paper

Title Page

Abstract | Introduction

Conclusions | References

Tables | Figures

◄ | ►|

◄ | ►

Back | Close

Full Screen / Esc

Printer-friendly Version

Interactive Discussion

Abstract

The composition and physical properties of aged atmospheric aerosol were characterized at a remote sampling site on the northern coast of Crete, Greece induring the Finokalia Aerosol Measurement Experiment in May 2008 (FAME-2008). A reduced Dry-Ambient Aerosol Size Spectrometer (DAASS) was deployed to measure the aerosol water content and volumetric growth factor of fine particulate matter. The particles remained wet even at relative humidity (RH) as low as 20%. The aerosol was acidic during most of the measurement period, which likely contributed to the water uptake at low RH. The water content observations were compared to the thermodynamic model E-AIM, neglecting any contribution of the organics to aerosol water content. There was good agreement between the water measurements and the model predictions. Adding the small amount of water associated with the organic aerosol based on monoterpene water absorption did not change the quality of the agreement. These results strongly suggest that the water uptake by aged organic aerosol is relatively small (a few percent of the total water for the conditions of FAME-08) and generally consistent with what has been observed in laboratory experiments. The Q-AMS water concentration was well correlated with the DAASS measurements and in good agreement with the predicted values for the RH of the Q-AMS inlet. This suggests, that at least for the conditions of the study, the Q-AMS can provide valuable information about the aerosol water concentrations if the sample is not dried.

1 Introduction

Water uptake by atmospheric particles affects their size, lifetime, and optical and chemical properties. This can influence their interaction with climate, their deposition inside the humid respiratory tract and corresponding health effects (Martonen and Zhang, 2003; Löndahl et al., 2008), effects on visibility (Malm and Day, 2001; Sequeira and Lai, 1998), and it can change their lifetime and transport due to altered deposition

rates (Kreidenweis et al., 2001; Spichtinger and Cziczo, 2008).

Atmospheric aerosol can exist in multiple thermodynamically stable and metastable states. For simple salt systems a dry particle will uptake water at a critical relative humidity (RH), called the deliquescence point (DRH), grow suddenly, and then continue
5 to grow as RH is increased further. On the return branch of decreasing RH the salt particle can exhibit a hysteresis behavior by not following the same path but retaining water past the DRH until it crystallizes and collapses to its dry size at a lower RH known as the efflorescence point (ERH). For simple inorganic salts the deliquescence and efflorescence points are well known (Tang, 1997; Seinfeld and Pandis, 2006).
10 The behavior of complex mixtures including several organic components is not well understood, making it difficult to predict the liquid water concentrations of atmospheric particles. For RH less than 80% or so it is not clear if the ambient particles are liquid droplets or dry particles.

The hygroscopic tandem differential mobility analyzer (H-TDMA) is one tool often
15 used to measure hygroscopic growth of ambient particles (Berg et al., 1998; Cocker et al., 2001; Nilsson, 2009). The H-TDMA size selects a nearly monodisperse stream of dried aerosol, exposes the size-selected particles to an elevated RH and then measures the resultant size distribution, and thus growth, with a scanning mobility particle sizer (SMPS). One of the major limitations of the H-TDMA comes from most mea-
20 surements occurring at 90% RH, limiting the ability to explore metastable states and deliquescence behaviors which would be observed at lower RH (Swietlicki et al., 2007). When an H-TDMA is used to scan RH it can reveal particle state information. For example, measurements at Jungfraujoch, which is a ground-based station representative of conditions in the free troposphere, were taken in the range of 10–85% RH without
25 evidence of efflorescence behavior (Weingartner et al., 2002; Sjogren et al., 2008). Choi and Chan (2002) have shown that organic components have the potential to delay or inhibit efflorescence, but a lack of efflorescence is also consistent with sulfate aerosols that are not fully neutralized.

Some H-TDMA studies have found evidence that organic components are hygroscopic (Dick et al., 2000) while others have shown that organics can impact the water uptake both positively and negatively for non-urban and urban sampling locations, respectively (Saxena et al., 1995). One study sought to isolate the less hydrophilic organic fraction of ambient continental-rural aerosol in Hungary (Gysel et al., 2004). The hygroscopic diameter growth factor ($D_{p,\text{wet}}/D_{p,\text{dry}}$) of the less hydrophilic component ranged from 1.08 to 1.17, which is comparable to smog-chamber secondary organic aerosol measurements of 1.1 at 85% RH (Virkkula et al., 1999).

Despite the many contributions of H-TDMA measurements, this technique lacks the ability to measure liquid water content of atmospheric particles in their ambient state. This is because the particles are dried prior to sampling, and then re-wetted. Other approaches have been used to estimate the liquid water content of ambient particles and sometimes to attempt to constrain the contribution of organic material to the liquid water content. Chemical analysis combined with filters weighed at varying RH have been used to determine the amount of water attributable to the inorganic constituents in filter samples from Research Triangle Park, North Carolina. The excess liquid water (about 20%) was attributed to the organic compounds (Speer et al., 2003). Other researchers have used a nephelometer, comparing the scattering at ambient RH to the scattering at a reduced RH (Covert et al., 1979). This method was used in several national parks and found that particles retained water to very low RH at some locations (Great Smoky Mountains and Big Bend), whereas evidence of efflorescence was observed at the Grand Canyon (Malm et al, 2000; Malm and Day, 2001; Malm et al., 2003). This work also suggested that organic aerosols were weakly hygroscopic.

The Dry-Ambient Aerosol Size Spectrometer (DAASS) was developed to make direct in situ measurements of the water content of the entire distribution of ambient aerosols (Stanier et al., 2004). The DAASS was deployed for field monitoring during the Pittsburgh supersite, where a seasonal deliquescence behavior was observed as well as an increased water uptake due to the organic component of the aerosol (Khlystov et al., 2005). Its major advantage is that it measures the aerosol water concentration of

the full $PM_{0.5}$, PM_1 or PM_{10} distribution and does not focus on the behavior of particles of a given size like the H-TDMA. It also characterizes the particles in their ambient state without the need to first dry them and then expose them to higher RH. Finally, the reduced DAASS requires only one DMA compared to the two needed by the H-TDMA.

Despite the known importance of water uptake in ambient aerosol systems there is a relative dearth of water measurements, and our comprehension is hampered by complexities of unknown organics combined with inorganic systems. In this work a reduced DAASS system is deployed for monitoring remote ambient aerosols in the critical size range of 10 to 500 nm at ambient and low (<25%) RH. Additionally, a Q-AMS is used to monitor undried atmospheric particles. The goal is to determine the state, water content, and volume growth factors of the particles and compare the observations to existing models for inorganic components in order to increase our understanding of the impact of organics on the complex atmospheric mixtures.

2 Experimental

2.1 Sampling site

Measurements were taken at the Finokalia station (35° 24′ N, 25° 60′ E) on the northeast coast of the island of Crete. The sampling station is located at a 250 m elevation far from any major local anthropogenic sources; the closest urban center is Heraklion, which is approximately 50 km to the west. The island's location in the Eastern Mediterranean makes it an ideal location for sampling a variety of air masses that have been transported to Crete, including marine, African and European outflows. Further details of the sampling site are reported elsewhere (Mihalopoulos et al., 1997; Kouvarakis et al., 2000; Sciare et al., 2003).

Title Page

Abstract | Introduction

Conclusions | References

Tables | Figures

◄ | ►

◄ | ►

Back | Close

Full Screen / Esc

Printer-friendly Version

Interactive Discussion

2.2 Instrumentation

The Finokalia Aerosol Measurement Experiment from May to June 2008 (FAME-08) was part of the European Integrated Project on Aerosol Cloud Climate and Air Quality Interactions (EUCARRI) intensive campaign occurring throughout Europe during May
5 2008 (Kulmala et al., 2009). An overview of the FAME-08 field mission with details on each of the measurements described below has been presented by Pikridas et al. (2010). The present work focuses on measurements related to water uptake and our theoretical understanding of particulate water.

2.2.1 Dry-ambient aerosol size spectrometer

10 The DAASS consists of a scanning mobility particle sizer (SMPS, TSI 3936L), automated valves, and a particle conditioning system that measures aerosol number distributions at ambient RH and at low RH. A schematic is shown in Fig. 1. This is a reduced system based upon the design of Stanier et al. (2004). The SMPS is operated at a sheath to aerosol ratio of 5:1 lpm for a mobility diameter size range of particle mea-
15 surement from approximately 10 to 500 nm. Particles are equilibrated to a Boltzmann charge distribution with a [85]Kr neutralizer (TSI, 10 mCi 3077a). Each SMPS upscan is 5 min in duration followed by a 5-min downscan. The DAASS has two sampling modes, dried and ambient, and a vent mode (Fig. 1). The difference between the ambient and dry mode aerosol volume distributions is equal to the particulate water concentration.
20   In the dried sampling mode, the particles were passed through a modified inlet including a single-tube Nafion dryer in a stainless steel casing (Permapure MD-110, Toms River, NJ). The sheath air in the SMPS was also dried in a closed loop. Since the sheath line required a higher flow rate a multi-tube Nafion dryer (Permapure PD-50T) was used. Dry air (Fig. 1) for the countercurrent streams of the Nafion dryers was pro-
25 vided at a rate of 5 lpm for the inlet dryer and 15 lpm for the sheath dryer by an oil-free compressor and a heatless dryer (not shown in Fig. 1; Permapure HD-2000) with final polishing via a carbon cap, silica gel dryer and a HEPA filter.

Title Page

Abstract | Introduction

Conclusions | References

Tables | Figures

◄ | ►I

◄ | ►

Back | Close

Full Screen / Esc

Printer-friendly Version

Interactive Discussion

In the ambient mode the Nafion dryers were bypassed using three-way solenoid valves (Alcon U33-42-21-12, Itasca, IL, USA). This operation was akin to a traditional SMPS measurement. After the ambient-mode scan ended the system was prepared for dry sampling in what is termed the dry preparation. This meant the automated valves entered the dry configuration, but size distribution data were not being collected to allow for system stabilization.

The third flow mode, a vent stage, rapidly prepared the system to switch from the dried sampling mode to the ambient sampling mode by operating in a once-through flow configuration (Fig. 1) in which dried air was exhausted and ambient air was drawn into the system. This air exchange was aided by a pump to drive a greater amount of air through the system without straining the SMPS blowers. One minute prior to the end of the vent mode the system was returned to a recirculating flow for the SMPS blowers to stabilize.

Maintaining the ambient temperature throughout the system was critical to sampling at ambient RH, so all of the instrumentation was placed outdoors. The DAASS system was shielded from sunlight by a large weatherproof canopy. In order to increase air flow around the system a fan was placed at the end of the canopy. Relative humidity and temperature were measured at three points in the DAASS (ambient at the entrance to DAASS, after the inlet dryer/bypass, and at the exit of the differential mobility analyzer column before the condensation particle counter (CPC, TSI 3772)). The RH data were logged by the LabView software, which also controlled the valves (Fig. 1).

As atmospheric particles lose water they shrink. However, the maximum mobility diameter measured by the SMPS is constant and determined by the sheath flow rate and maximum voltage applied to the DMA column. As the aerosol is dried in the DAASS, additional particles enter the measurable sampling window. In order to determine the amount of water taken up by the particles we must apply a small correction for this sampling bias to exclude the additional particles in the dry distribution. Using the method of Stanier et al. (2004) the total measured volumes of the ambient and dry distributions

Water content of aged aerosol

G. J. Engelhart et al.

are:

$$V_{\text{dry}} = \frac{\pi}{6} \int_{D_{d1}}^{D_{d2}} D^3 n_{\text{dry}}(D) dD \tag{1}$$

$$V_{\text{ambient}} = \frac{\pi}{6} \int_{D_{a1}}^{D_{a2}} D^3 n_{\text{ambient}}(D) dD \tag{2}$$

where V_{ambient} is the total ambient particle volume concentration, D is the particle mo-
bility diameter, D_{a1} and D_{a2} are the upper and lower integration limits, respectively, of
the ambient distributions, and $n(D)$ is the aerosol number distribution. To obtain V_{dry},
the upper integration limit, D_{d2}, is adjusted so that the same number of particles are
considered in both the ambient and dry distributions. This means that the upper inte-
gration limit for the dry distribution will be lower than that of the ambient distribution.
While the lower integration limits, D_{d1} and D_{a1}, will be impacted by the same distri-
bution shift we will neglect this for two reasons. First, very few particles smaller than
15 nm were present during FAME-08 (Pikridas et al., 2010). Second, the smallest parti-
cles in the distribution contribute little volume and therefore do not introduce significant
error if neglected. We define the volume growth factor as:

$$\text{VGF} = \frac{V_{\text{ambient}}}{V_{\text{dry}}} = \frac{\int_{D_{a1}}^{D_{a2}} D^3 n_{\text{ambient}}(D) dD}{\int_{D_{d1}}^{D_{d2}} D^3 n_{\text{dry}}(D) dD} \tag{3}$$

If we assume that the aged submicrometer particle population was homogeneous
and therefore all the particles have the same growth factor then:

$$\text{VGF} = \left(\frac{D_{a2}}{D_{d2}}\right)^3 \tag{4}$$

Iteration is used to find the size boundary D_{d2} which simultaneously satisfies Eqs. (3) and (4). The corresponding VGF then accounts for the differences between the ambient and dried distributions. Once the integration limit for the dry distribution has been determined the aerosol water concentration (for particles with diameter smaller than approximately 500 nm) can be found by:

$$m_w = \rho_w(V_{\text{ambient}} - V_{\text{dry}}) \tag{5}$$

where ρ_w is the density of water.

2.2.2 Aerosol mass spectrometer

A Quadrupole Aerosol Mass Spectrometer (Q-AMS, Aerodyne Research, Inc.) continuously measured the chemical composition of submicrometer non-refractory aerosol including sulfate, organics, nitrate, and ammonium. The Q-AMS operation alternated between sampling mass spectral information for mass to charge (m/z) ratios between 1 and 300 and sampling particle time of flight (pToF) aerodynamic size information every 15 s. The Q-AMS was located in an air-conditioned room and particles were sampled through a PM_{10} sampling head positioned on the roof. The Q-AMS vaporizer was set at 600 °C to rapidly volatilize ammonium sulfate and any other non-refractory compounds that would flash-vaporize below 600 °C, as is typical for standard use of the instrument. Black carbon and other refractory compounds cannot be measured by this type of AMS. The measurements were analyzed with a standard batch and fragmentation table (Allan et al., 2004) with some minor modifications as described in Hildebrandt et al. (2010).

In this campaign the aerosol was sampled directly without drying of the sample. It has been shown that some particle water may evaporate in the AMS aerodynamic lens (Murphy, 2007); consequently the AMS is not typically used for particle water measurements. Our objective is to establish a reliable protocol for using the AMS to measure particulate water. Determining the PM water with the Q-AMS requires careful adjustments to the standard Q-AMS fragmentation table to account for changes

with absolute humidity. The challenge is to separate the gas-phase water signal from the total water signal at m/z 18 so that the remaining water can be attributed to the particles. We make the assumption that the gas-phase ratio of H_2O^+/N_2^+ scales with absolute humidity. In the pToF spectra of the AMS, gas-phase species appear well
5 before the particle-phase species; this can be used to separate the gas and particle-phase signals via integration of only the gas-phase signal. Due to inherent signal noise in the pToF distribution, the data was binned by absolute humidity and averaged before integration. For more details on this procedure, see Hildebrandt et al. (2010). The default relative ionization efficiency of water of 1 was used, which to our knowledge is
10 used in all Q-AMS analysis.

3 Results and discussion

3.1 Instrument performance

Figure 2 shows a typical time series of RH throughout the DAASS flow configurations. The sheath RH is low during the dry sampling period. As the dry period ends, the
15 valves switch to the vent mode where ambient air is rapidly drawn into the system causing a rapid increase in the RH. The relative humidity does not reach ambient conditions during the very rapid once-through vent flow, but quickly returns to near ambient RH when the valves switch to recirculating flow and allow the SMPS blowers and RH sensors to stabilize. After stabilization the ambient sample is measured for 5 min before
20 the system enters the dry configuration. Here a rapid decrease in RH is observed. This is the "dry preparation" period during which size distribution data are not collected, but the system equilibrates to the low RH in preparation for the dry sampling period (which starts the repeating sequence). The instrument cycles through these flow modes collecting both ambient and dried particle distribution information.
25   During FAME-08 the sheath RH tracked the ambient RH fairly closely (Fig. 3). During the ambient sampling mode, the RH monitor located after the inlet measured RH a few

Full Screen / Esc

Printer-friendly Version

Interactive Discussion

percent lower than ambient, potentially due to some heating from the solenoid valves. However, the particles rapidly equilibrated at the RH of the sheath air and this RH was used as the reference RH for the ambient measurement (Stanier et al., 2004). The dry relative humidity was lower than 25% even for the highest ambient RH conditions. The ambient RH during most of the study (approximately 90% of the time) was less than 70%. During the brief periods when the RH was high there were significant differences between the recorded RH values, so our analysis will focus on the data below 70% ambient RH.

3.2 DAASS Water

The particles during FAME-08 showed no signs of efflorescence (Fig. 4). The particles retained as much as 10% of their total particulate volume in water at 20% RH. At 50% RH, where particulate matter mass is often measured in the European monitoring networks (Tsyro et al., 2005) the particles still contained approximately 40% water by volume. One potential explanation for the persistent liquid state of the particles is the acidity of the particles. Water retention has also been observed for acidic aerosols in Pittsburgh and Switzerland (Khlystov et al., 2005; Fisseha et al., 2006). Figure 5 shows the acidity ratio for submicrometer particles as calculated from AMS concentrations for the time periods of DAASS measurement. The acidity ratio is calculated according to:

$$\text{Acidity Ratio} = \frac{\text{mol}_{NH_4^+}}{2 \cdot \text{mol}_{SO_4^{2-}} + \text{mol}_{NO_3^-}} \tag{6}$$

where $\text{mol}_{NH_4^+}$, $\text{mol}_{SO_4^{2-}}$ and $\text{mol}_{NO_3^-}$ are moles of ammonium, sulfate, and nitrate, respectively. Other species such as sodium chloride and dust were negligible in the size range of interest during FAME-08 (Pikridas et al., 2010). Acidity is not the only potential explanation, as deliquescence and efflorescence behavior has been shown to be inhibited for model aerosols by a number of organic components (Marcolli and Krieger, 2006).

3.3 Comparison to AMS water

Despite the potential loss of water from the particles in the aerodynamic lens of the AMS, we observe a strong correlation between measured DAASS water and measured AMS water. Figure 6 shows the data binned by every $0.5 \, \mu g \, m^{-3}$ according to the DAASS water. 95% of the DAASS water measurements were below $5.5 \, \mu g \, m^{-3}$ and the highest two data points for DAASS water represent only 3 h over the entire campaign. The trend line is a weighted linear fit to the data and given by:

$$(\text{AMS Water}) = 0.44 \, (\text{DAASS Water}) + 0.74 \, \mu g \, m^{-3} \tag{7}$$

The Q-AMS was located inside a room controlled to a temperature around 25 °C throughout the campaign as opposed to the DAASS, which was located outside under ambient conditions. The sampling lines leading to the Q-AMS were sufficiently long for the sample to come into equilibrium with the room temperature, altering the RH from ambient conditions. This may explain some of the observed disagreement at high water content, as water content versus RH is exponential in nature. We will explore this in a subsequent section using thermodynamic theory. Other potential reasons for the discrepancy include the slightly different size ranges measured by the two systems and the Q-AMS water measurement itself. The Q-AMS analysis uses the standard batch table, which includes a relative ionization efficiency (RIE) of water equal to 1 with respect to nitrate (Jimenez et al., 2003; Allen et al., 2004). If this value is not truly equal to 1 it will introduce error into the water mass calculation, either enhancing or somewhat offsetting the effect of water evaporation in the aerodynamic lens.

3.4 Comparison to thermodynamic theory

The inorganic concentrations for sulfate, ammonium, and nitrate measured by the Q-AMS were used as inputs into the Extended Aerosol Inorganic Model II (E-AIM, http://www.aim.env.uea.ac.uk/aim/aim.php; Carslaw et al., 1995; Clegg et al., 1998; Massucci et al., 1999) in conjunction with the DAASS sheath RH and the sheath tem-

perature. The DAASS RH and temperature were averaged over the sampling interval of the Q-AMS. Production of all solids by the E-AIM model was suppressed and organic particulate related water was neglected. Similar calculations were conducted with E-AIM Model III, which allows for additional inorganic components but restricts the temperature calculation to 298.15 K. The resultant changes to aqueous water were negligible, so all calculations presented here employ Model II. The predicted VGF is calculated according to:

$$VGF_{Predicted} = \frac{\dfrac{m_{SO_4^{2-}}+m_{H^+}+m_{NH_4^+}}{\rho_{(NH_4)_2SO_4}} + \dfrac{m_{org}}{\rho_{org}} + \dfrac{m_{NO_3^-}}{\rho_{NO_3}} + \dfrac{m_{H_2O_{aq}}}{\rho_{H_2O}}}{\dfrac{m_{SO_4^{2-}}+m_{H^+}+m_{NH_4^+}}{\rho_{(NH_4)_2SO_4}} + \dfrac{m_{org}}{\rho_{org}} + \dfrac{m_{NO_3^-}}{\rho_{NO_3}} + \dfrac{m_{lowRHH_2O_{aq}}}{\rho_{H_2O}}} \qquad (8)$$

where m_i and ρ_i are the mass and density of the given species. The organic aerosol density during FAME-08 was determined to be approximately 1.35 µg m^{-3} by comparing the Q-AMS mass distribution to the SMPS size distribution measurements (Lee et al., 2010; Kostenidou et al., 2007). We use the ammonium sulfate density for both ammonium bisulfate and sulfate and also take advantage of the fact that there was very little nitrate during the study (Pikridas et al., 2010).

In order to compare the DAASS measurements to E-AIM theoretical calculations, Model II was used to simulate the low RH conditions of the sheath air to estimate the amount of water remaining during the low RH conditions. This correction was minor (around 6%), but non-negligible. Particles were assumed to have negligible water below 10% RH.

The time series of the predicted and the measured aerosol water is shown in Fig. 7. The theory seems to reproduce the measurement time series well even if the water content of the organics is neglected in this calculation.

The impact of organics on water uptake is still largely unknown. We use corrected UNIFAC predictions of water uptake from Koo et al. (2003) for α-pinene oxidation products as a surrogate for our organic compounds. The concentration of organics was supplied from the Q-AMS. The estimated contribution of aerosol water associated with

organics is small, especially compared with the contribution of water associated with inorganics at the same RH. The organic associated water has a small impact on the predicted VGF, a 3% average increase with the addition of organic water, shown in Fig. 8. Therefore, the measured DAASS water is consistent with a relatively small water uptake of organics.

We can use the same thermodynamic theory to determine the amount of water predicted under Q-AMS measurement conditions. Measurements of ambient temperature and RH are used to calculate the absolute humidity of the sample at the Q-AMS inlet. An indoor temperature measurement is then used to calculate the RH corresponding to the absolute humidity of the ambient sample. E-AIM is used to predict the particulate water content at these RH conditions using the same chemical composition information as before. The predictions are compared to the Q-AMS measurements of particulate water in Fig. 9. The agreement is striking. The predictions and measurements do not agree well on 21 May, which was an unusual day due to high concentrations of dust in the outflow from Africa. We disregard this day of measurements to find a correlation of:

$$\text{(AMS Water)} = 0.77 \text{ (Predicted Water)} + 0.43 \, \mu\text{g m}^{-3} \tag{9}$$

This correlation has an R^2 value of 0.73. If we assume a zero intercept the correlation becomes:

$$\text{(AMS Water)} = 1.03 \text{ (Predicted Water)} \tag{10}$$

This correlation has an R^2 value of 0.72. However, as both the DAASS–AMS comparison shown in Fig. 6 and the E-AIM–AMS comparison shown in Fig. 9 show a small positive intercept in aerosol water measured by the Q-AMS, it is possible that the standard fragmentation table employed in this analysis slightly underestimates the water ion signal arising from fragmentation of either hydrated inorganic or oxygenated organic compounds.

4   Conclusions

The aged aerosols sampled during the FAME-08 field mission on Crete were wet throughout the entire sampling period. This lack of efflorescence may be aided by the acidity of the particles that was common throughout the study. Additionally, our understanding of inorganic water uptake and organic water uptake reproduce the measurement data well. Even when they are very aged, organics absorb a relatively small amount of particulate water, increasing total particulate water in this sulphur rich environment by only a few percent. The E-AIM model for inorganics predictions is consistent with the DAASS measurements. Interestingly, we find a strong correlation between the particle water content measured by the DAASS and by the Q-AMS. Predictions of the particle water content for the measurement conditions of the Q-AMS agree with Q-AMS measurements quite well. This is a promising result for rapidly increasing our understanding of water in atmospheric particulate matter and should be considered in experimental design for future field missions.

References

Allan, J. D., Delia, A. E., Coe, H., Bower, K. N., Alfarra, M. R., Jimenez, J. L., Middlebrook, A. M., Drewnick, F., Onasch, T. B., Canagaratna, M. R., Jayne, J. T., and Worsnopf, D. R.: A generalised method for the extraction of chemically resolved mass spectra from Aerodyne aerosol mass spectrometer data, J. Aerosol Sci., 35, 909–922, doi:10.1016/j.jaerosci.2004.02.007, 2004.

Berg, O. H., Swietlicki, E. and Krejci, R.: Hygroscopic growth of aerosol particles in the marine boundary layer over the Pacific and Southern Oceans during the First Aerosol Character-

ization Experiment (ACE 1), J. Geophys. Res., 103(D13), 16535, doi:10.1029/97JD02851, 1998.

Carslaw, K. S., Clegg, S. L. and Brimblecombe, P.: A thermodynamic model of the system $HCl-HNO_3-H_2SO_4-H_2O$, including solubilities of HBr, from <200 K to 328 K. J. Phys. Chem., 99, 11557–11574, 1995.

Choi, M. Y. and Chan, C. K.: The effects of organic species on the hygroscopic behaviors of inorganic aerosols, Environ. Sci. Technol., 36, 2422–2428, 2002.

Clegg, S., Brimblecombe, L. P., and Wexler, A. S.: A thermodynamic model of the system $H^+-NH_4^+-SO_4^{2-}-NO_3^--H_2O$ at tropospheric temperatures, J. Phys. Chem. A102, 2137–2154, doi:10.1021/jp973043j, 1998.

Cocker, D. R., Whitlock, N. E., Flagan, R. C., and Seinfeld, J. H.: Hygroscopic properties of Pasadena, California aerosol. Aerosol. Sci. Tech. 35, 637–647, doi:10.1080/02786820120653, 2001.

Covert, D. S., Waggoner, A. P., Weiss, R. E., Ahlquist, N. C., Charlson, R. J.: Atmospheric aerosols, humidity and visibility, in: Character and Origins of Smog Aerosols, edited by: Hidy, G. M., Mueller, P. K., Grosjean, D., Appel, B. R., Weslowski, J. J., Wiley, New York, USA, 559–581, 1979.

Dick, W. D., Saxena, P., and McMurry, P. H.: Estimation of water uptake by organic compounds in submicron aerosols measured during the Southeastern aerosol and visibility study, J. Geophys. Res., 105, 1471–1479, doi:10.1029/1999JD901001, 2000.

Fisseha, R., Dommen, J., Gaeggeler, K., Weingartner, E., Samburova, V., Kalberer, M., and Baltensperger, U.: Online gas and aerosol measurement of water soluble carboxylic acids in Zurich, J. Geophys. Res., 111, D12316, doi:10.1029/2005JD006782, 2006.

Gysel, M., Weingartner, E., Nyeki, S., Paulsen, D., Baltensperger, U., Galambos, I., and Kiss, G.: Hygroscopic properties of water-soluble matter and humic-like organics in atmospheric fine aerosol, Atmos. Chem. Phys., 4, 35–50, doi:10.5194/acp-4-35-2004, 2004.

Hildebrandt, L., Engelhart, G.J., Mohr, C., Kostenidou, E., Bougiatioti, A., DeCarlo, P. F., Prevot, A. S. H., Baltensperger, U., Mihalopoulos, N., Donahue, N. M., and Pandis, S. N.: Aged organic aerosol in the Eastern Mediterranean: The Finokalia Aerosol Measurement Experiment – 2008, Atmos. Chem. Phys., doi:10.5194/acp-10-4167-2010, 2010.

Jimenez, J. L., Jayne, J. T., Shi, Q., Kolb C. E., Worsnop D. R., Yourshaw, I., Seinfeld, J. H., Flagan, R. C., Zhang, X., Smith K. A., Morris, J. W., and Davidotis, P.: Ambient Aerosol Sampling with an Aerosol Mass Spectrometer, J. Geophys. Res. 108, 8425,

doi:10.1029/2001JD001213, 2003.

Khlystov, A., Stanier, C. O., Takahama, S., and Pandis, S. N.: Water content of ambient aerosol during the Pittsburgh Air Quality Study, J. Geophys. Res., 110, D07S10, doi:10.1029/2004JD004651, 2005.

Koo, B., Ansari, A. S., and Pandis, S. N.: Integrated approaches to modeling the organic and inorganic atmospheric aerosol components, Atmospheric Environment, 37, 4757-4768, doi:10.1016/j.atmosenv.2003.08.016, 2003.

Kostenidou, E., Pathak, R. K., and Pandis, S. N.:An algorithm for the calculation of secondary organic aerosol density combining AMS and SMPS data, Aerosol Sci. Technol., 41, 1002–1010, doi:10.1080/02786820701666270, 2007.

Kouvarakis, G., Tsigaridis, K., Kanakidou, M., and Mihalopoulos, N.: Temporal variations of surface regional background ozone over Crete Island in the Southeast Mediterranean, J. Geophys. Res., 105, 399–407, doi:10.1029/1999JD900984, 2000.

Kreidenweis, S. M., Remer, L. A., Bruintjes, R., and Dubovik, O.: Smoke aerosol from biomass burning in Mexico: Hygroscopic smoke optical model, J. Geophys. Res., 106, 4831–4844, doi:10.1029/2000JD900488, 2001.

Kulmala, M., Asmi, A., Lappalainen, H. K., Carslaw, K. S., Pöschl, U., Baltensperger, U., Hov, Ø., Brenquier, J.-L., Pandis, S. N., Facchini, M. C., Hansson, H.-C., Wiedensohler, A., and O'Dowd, C. D.: Introduction: European Integrated Project on Aerosol Cloud Climate and Air Quality interactions (EUCAARI) – integrating aerosol research from nano to global scales, Atmos. Chem. Phys., 9, 2825–2841, doi:10.5194/acp-9-2825-2009, 2009.

Lee, B. H., Kostenidou, E., Hildebrandt, L., Riipinen, I., Engelhart, G. J., Mohr, C., DeCarlo, P. F., Mihalopoulos, N., Prevot, A. S. H., Baltensperger, U., and Pandis, S. N.: Measurement of the ambient organic aerosol volatility distribution: Application during the Finokalia Aerosol Measurement Experiment (FAME- 2008), Atmos. Chem. Phys. Discuss., 10, 17435–17466, doi:10.5194/acpd-10-1-2010, 2010.

Löndahl, J., Pagelsb, J., Bomanc, C., Swietlickia, E., Masslinga, A., Risslerad, J., Blomberge, A., Bohgardb, M., and Sandstroumlme, T.: Deposition of biomass combustion aerosol particles in the human respiratory tract, Inhal. Toxicol., 40, 923–933, doi:10.1080/08958370802087124, 2008.

Malm, W. C. and Day, D. E.: Estimates of aerosol species scattering characteristics as a function of relative humidity, Atmos. Environ., 35, 2845–2860, doi:10.1016/S1352-2310(01)00077-2, 2001.

Malm, W. C., Day, D. E., and Kreidenweis, S. M.: Light scattering characteristics of aerosols as a function of relative humidity: Part I – a comparison of measured scattering and aerosol concentrations using the theoretical models, J. Air Waste Manage. Assoc., 50, 686–700, 2000.

Malm, W. C., Day, D. E., Kreidenweis, S. M., Collett Jr., J. L., and Lee, T.: Humidity dependent optical properties of fine particles during the Big Bend regional aerosol and visibility study (BRAVO), J. Geophys. Res., 108, 4279, doi:10.1029/2002JD002998, 2003.

Marcolli, C. and Krieger, U. K.: Phase changes during hygroscopic cycles of mixed organic/inorganic model systems of tropospheric aerosols, J. Phys. Chem., A110, 1881–1893, doi:10.1021/jp0556759, 2006.

Martonen, T. B. and Zhang, Z.: Deposition of Sulfate Acid Aerosols in the Developing Human Lung, Inhal. Toxicol., 5, 165–187, doi:10.3109/08958379309034500, 1993.

Massucci, M., Clegg, S. L., and Brimblecombe, P.: Equilibrium partial pressures, thermodynamic properties of aqueous and solid phases, and Cl_2 production from aqueous HCl and HNO_3 and their mixtures, J. Phys. Chem. A 103, 4209–4226, doi:10.1021/jp9847179, 1999.

Mihalopoulos, N., Stephanou, E., Kanakidou, M., Pilitsidis, S., and Bousquet, P.: Tropospheric aerosol ionic composition in the Eastern Mediterranean region, Tellus B-Chem. Phys. Meteorol., 49, 314–326, doi:10.1034/j.1600-0889.49.issue3.7.x, 1997.

Murphy, D.: The design of single particle laser mass spectrometers, Mass Spectrom. Rev., 26, 150–165, doi:10.1002/mas.20113, 2007.

Nilsson, E., Swietlicki, E., Sjogren, S., Löndahl, J., Nyman, M., and Svenningsson, B.: Development of an H-TDMA for long-term unattended measurement of the hygroscopic properties of atmospheric aerosol particles, Atmos. Meas. Tech., 2, 313–318, doi:10.5194/amt-2-313-2009, 2009.

Pikridas, M., Bougiatioti, K., Engelhart, G. J., Hildebrandt, L., Kostenidou, E., Mohr, C., Kouvarakis, G., Zarmpas, P., Psichoudaki, M., Gagne, S., Mihalopoulos, N., Pilinis, C., Hillamo, R., Baltensperger, U., Kulmala, M., and Pandis, S. N.: The Finokalia Aerosol Measurement Experiments – 2008 (FAME-08): An Overview, Atmos. Chem. Phys., doi:10.5194/acp-10-6793-2010, 2010.

Saxena, P., Hildemann, L. M., McMurry, P. H., and Seinfeld, J. H.: Organics alter hygroscopic behavior of atmospheric particles, J. Geophys. Res., 100, 18755–18770, doi:10.1029/95JD01835, 1995.

Sciare, J., Bardouki, H., Moulin, C., and Mihalopoulos, N.: Aerosol sources and their contri-

bution to the chemical composition of aerosols in the Eastern Mediterranean Sea during summertime, Atmos. Chem. Phys., 3, 291–302, doi:10.5194/acp-3-291-2003, 2003.

Seinfeld, J. H. and Pandis, S. N.: Atmospheric Chemistry and Physics – From Air Pollution to Climate Change (2nd Edition), John Wiley & Sons, 450–460, 2006.

5   Sequeira, R. and Lai, K. H.: The effect of meteorological parameters and aerosol constituents on visibility in urban Hong Kong, Atmos. Environ., 32, 2865–2871, doi:10.1016/S1352-2310(97)00494-9, 1998.

Speer, R. E., Edney, E. O., and Kleindienst, T. E.: Impact of organic compounds on the concentrations of liquid water in ambient $PM_{2.5}$, J. Aerosol Sci., 34, 63–77, doi:10.1016/S0021-
10   8502(02)00152-0, 2003.

Spichtinger, P. and Cziczo, D. J.: Aerosol–cloud interactions—a challenge for measurements and modeling at the cutting edge of cloud–climate interactions, Environ. Res. Lett. 3, 025002, doi:10.1088/1748-9326/3/2/025002, 2008.

Stanier, C. O., Khlystov, A. Y., Chan, W. R., Mandiro, M., and Pandis, S. N.: A method
15   for the in situ measurement of fine aerosol water content of ambient aerosols: The dry-ambient aerosol size spectrometer (DAASS), Aerosol Sci. Technol., 38, 215–228, doi:10.1080/02786820390229525, 2004.

Sjogren, S., Gysel, M., Weingartner, E., Alfarra, M. R., Duplissy, J., Cozic, J., Crosier, J., Coe, H., and Baltensperger, U.: Hygroscopicity of the submicrometer aerosol at the high-
20   alpine site Jungfraujoch, 3580 m a.s.l., Switzerland, Atmos. Chem. Phys., 8, 5715–5729, doi:10.5194/acp-8-5715-2008, 2008.

Swietlicki, E., Hansson, H.-C., Hämeri, K., Massling, A., Petäjä, T., Tunved, P., Weingartner, E., Baltensperger, U., McMurry, P.H., McFiggans, G., Svenningsson, B., Rissler, J., Wiedensohler, A., and Kulmala, M.: Hygroscopic properties of sub-micrometer atmospheric aerosol
25   particles measured with H-TDMA instruments in various environments – A review, Tellus B, 60, 353–364, doi:10.1111/j.1600-0889.2008.00350.x, 2007.

Tang, I. N.: Thermodynamic and optical properties of mixed-salt aerosols of atmospheric importance, J. Geophys. Res.-Atmos., 102, 1883–1893, doi:10.1029/96JD03085, 1997.

Tsyro, S. G.: To what extent can aerosol water explain the discrepancy between model calcu-
30   lated and gravimetric PM_{10} and $PM_{2.5}$?, Atmos. Chem. Phys., 5, 515–532, doi:10.5194/acp-5-515-2005, 2005.

Virkkula, A., Van Dingenen, R., Raes, F., and Hjorth, J.: Hygroscopic properties of aerosol formed by oxidation of limonene, alpha-pinene, and beta-pinene. J. Geophys. Res., 104,

3569–3579, doi:10.1029/1998JD100017, 1999.

Weingartner, E., Gysel, M., and Baltensperger, U.: Hygroscopicity of aerosol particles at low temperatures. 1. New low-temperature HTDMA instrument: setup and first applications, Environ. Sci. Technol. 36, 55–62, doi:10.1021/es010054o, 2002.

Water content of aged aerosol

G. J. Engelhart et al.

Title Page

Abstract	Introduction
Conclusions	References
Tables	Figures

|◄ | ►|

◄ | ►

Back | Close

Full Screen / Esc

Printer-friendly Version

Interactive Discussion
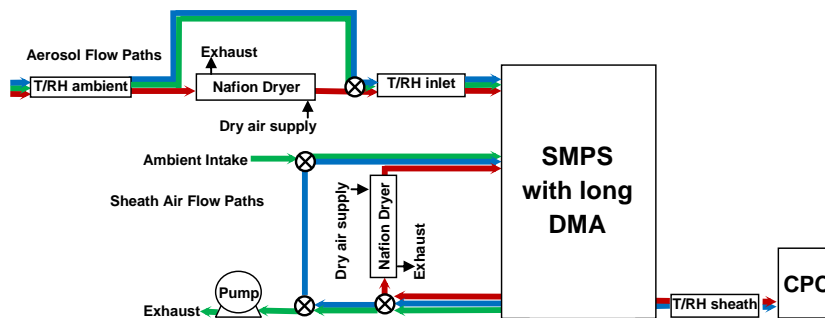
Fig. 1. Schematic of DAASS flow paths. Red is the dried sampling mode, blue is the ambient sampling mode and green is the vent mode.
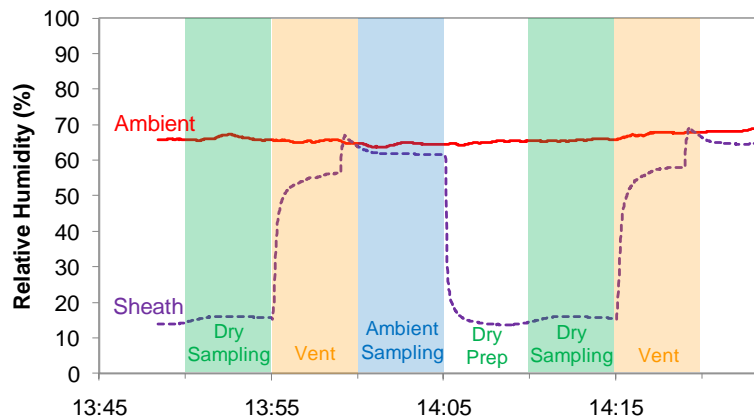
Fig. 2. Example of RH time series in DAASS for the various instrument modes.
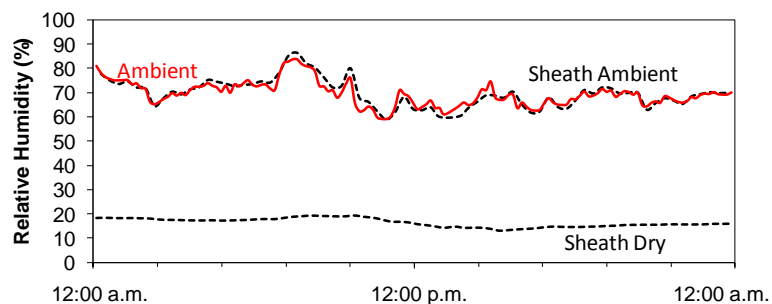
Fig. 3. Example data from midnight on 8 May to midnight on 9 May. Ambient RH (red) and sheath dry/ambient (black dashed).
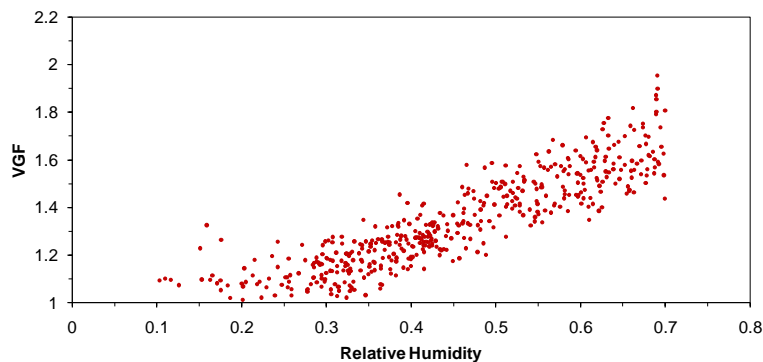
Fig. 4. Volume growth factor versus relative humidity for DAASS measurements with one hour averaging during FAME-08.
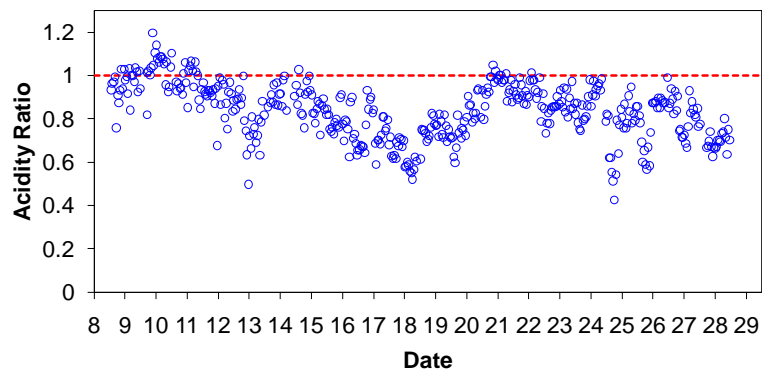
Fig. 5. Acidity ratio versus time as calculated from the molar ratio of ammonium over nitrate and sulfate as measured by the Q-AMS with one hour averaging.
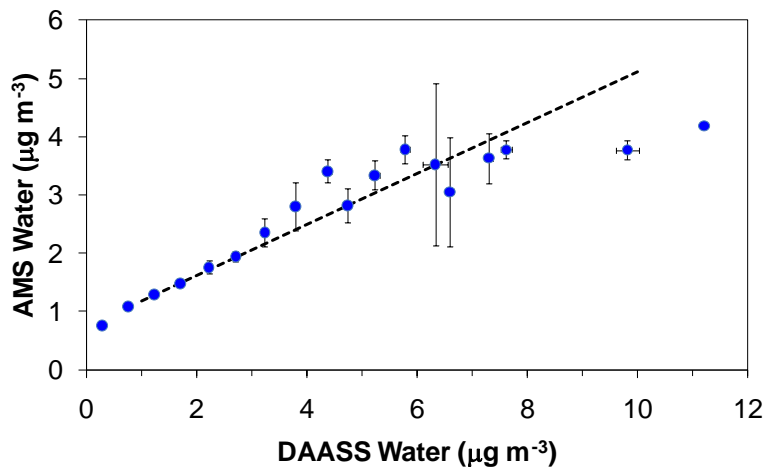
Fig. 6. DAASS water versus AMS water averaged for every $0.5\,\mu g\,m^{-3}$ bin in the DAASS water. Error bars reflect one standard deviation divided by the square root of the total number of samples in that size bin minus one.

Water content of aged aerosol

G. J. Engelhart et al.
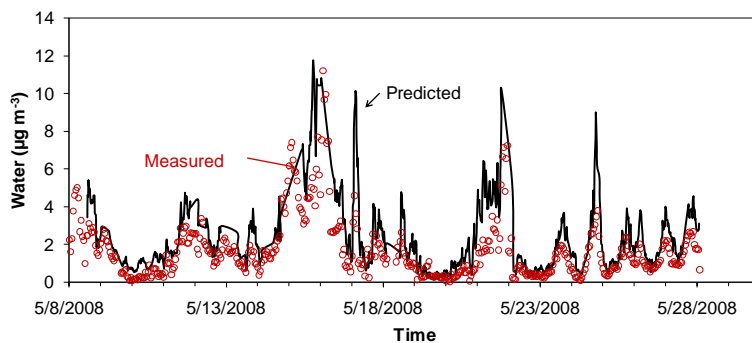
Fig. 7. Water versus time as calculated from E-AIM and measured by the DAASS.

Full Screen / Esc

Printer-friendly Version

Interactive Discussion
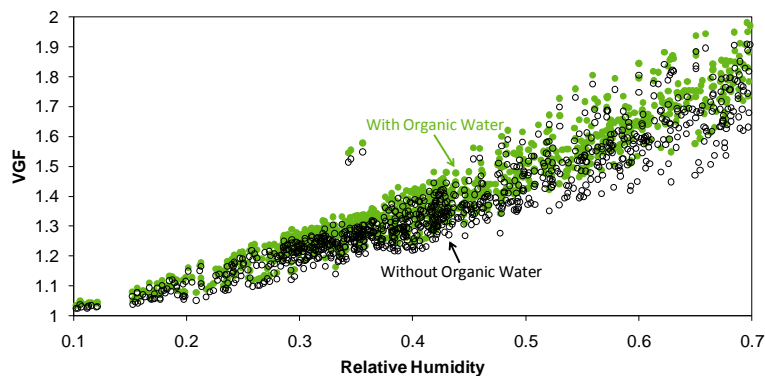
Fig. 8. Predicted volume growth factor versus RH predicted from the E-AIM model using only inorganics (black) and water uptake from organics estimated from Koo et al., 2003 (green).
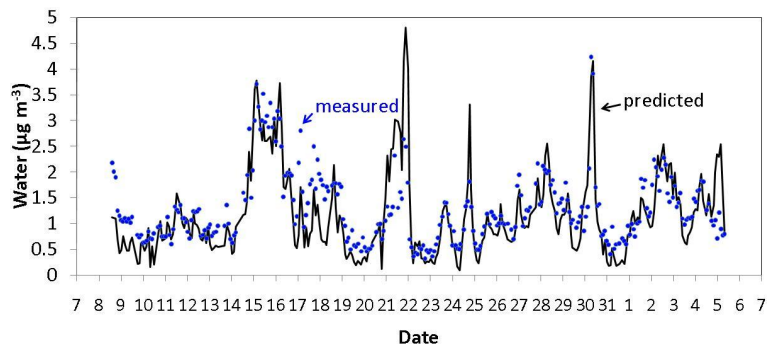
Fig. 9. Particulate water as measured by the AMS (blue points) versus predicted water (black line).